DOI: http://dx.doi.org/10.15407/tpwj2018.11–12.07

DIFFUSION WELDING AND BRAZING OF DISSIMILAR MATERIALS WITH CONTROLLED STRESS-STRAIN STATE

V.V. KVASNYTSKYI[1], **V.F. KVASNYTSKYI**[2], **CHEN HEXING**[3], **M.V. MATVIENKO**[2] and **G.V. YERMOLAYEV**[2]
[1]NTTU «Igor Sikorskii Kyiv Polytechnic Institute»
37 Prosp. Peremohy, 03056, Kyiv, Ukraine. E-mail: kvas69@ukr.net
[2]Adm. Makarov National Shipbuilding University
9 Heroiv Ukrainy Prosp., 54025, Mykolaiv, Ukraine. E-mail: welding@nuos.edu.ua
[3]Guangdong Academy of Sciences
No.9, Building, 100 Xianlie Rd. Guangzhou, P. R. China. E-mail: chenhexing@gdas.gd.cn

Stress-strain state in vacuum diffusion welding and brazing of dissimilar materials was studied, allowing for plastic deformations of instantaneous plasticity and creep. The role of plastic deformations in joint formation and residual stresses in vacuum diffusion welding of dissimilar metals, in particular of metals with nonmetals, as well as similar materials with interlayers is considered. Application of temperature loading simultaneously with external load at vacuum diffusion welding of dissimilar metals allows creating a bulk stressed state in the butt joint, with formation of axial, radial, circumferential, tangential stresses, promoting localization of plastic deformations in the butt joint zone and development of shear deformations, and intensification of the processes of formation of physical contact, activation of the surfaces and development of diffusion processes, respectively. Control of stress-strain state at joining of metals with nonmetals allows regulation of relaxation processes at cooling and prevention of joint fracture. 12 Ref., 9 Figures.

Keywords: *diffusion welding, brazing, stresses, strains, modeling, structure, mechanical properties, diffusion*

Manufacturing parts and components from dissimilar materials allows improvement of the performance of machines, devices and new equipment, as this enables combining the different properties of materials, which cannot be achieved in structures from similar materials. The range of materials used in combined structures, is quite diverse. New materials have been developed, for instance, composite materials, produced by powder metallurgy methods, high-temperature nickel casting superalloys, intermetallic materials and other, which cannot be heated up to melting temperature. In such cases solid-state welding, for instance, vacuum diffusion welding (VDW), friction welding, etc. are used [1]. Brazing is often applied, when joining metals to nonmetals, but problems related to the difference in physicomechanical properties (PMP) of the materials being joined and occurrence of residual stresses (RS) still remain [2, 3].

A problem in VDW of dissimilar materials is the nonuniformity of distribution of plastic deformations over the butt area, and, accordingly, also the processes of formation of physical contact, activation of the surfaces and bulk interaction (diffusion, recrystallization). In [3] we showed that VDW with thermal cycling is one of the promising methods for controlling the stress-strain state (SSS) and distribution of plastic deformations.

The objective of this work was improvement of the technology of VDW and brazing of dissimilar materials by controlling SSS formation, allowing for plastic deformations. Mechanics of joining in diffusion welding, brazing and spraying of dissimilar materials under the conditions of elasticity is considered in [4].

In order to establish the fundamental possibility of controlling the plastic deformations appearance in the zone of the butt joint of dissimilar materials and its regularities at VDW with thermal cycling, modeling of SSS in the most widely used assemblies of the type of cylinder-cylinder (C–C), bushing-bushing (B–B) and bushing-flange (B–F) was performed at heating and cooling for 100 °C. Finite element method and ANSYS software package were used for SSS modeling. Adequacy of modeling results was confirmed by analytical solutions and data derived by experimental method of speckle-interferometry, described in [5]. General view of the section of FE models of C–C, B–B and B–F assemblies is given in Figure 1.

Modeling of SSS of the assemblies allowing for plastic deformations of instantaneous plasticity showed that principal regularities of formation of SSS of cylindrical assemblies, established in [3, 4] for the elastic state, are preserved, but the stress level decreases considerably. At modeling, the moduli

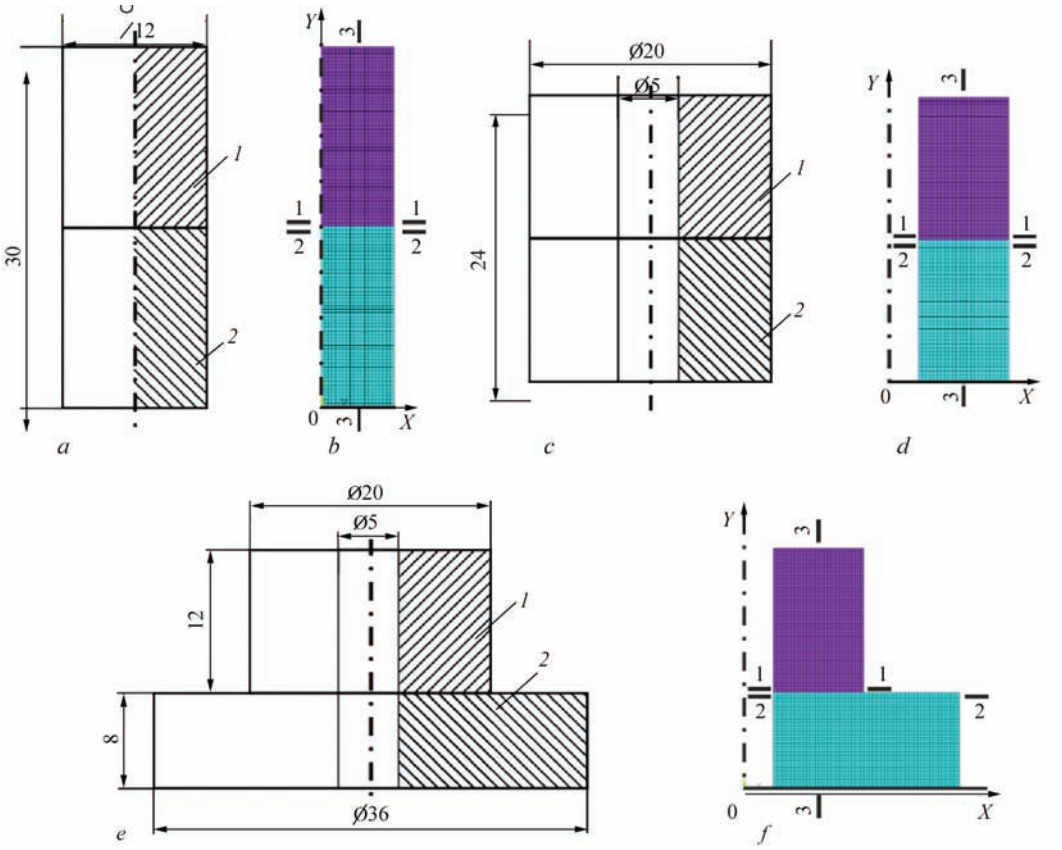

Figure 1. General view (*a–c*) in the section of FE models (*b*, *e*, *f*) of C–C, B–B, B–F assemblies, respectively

of elasticity were taken to be the same, yield limit in C–C and B–B assemblies was smaller in part *1*, in B–F assembly the yield limits are both the same, and smaller in the bushing or in the flange. Temperature coefficients of linear expansion (TCLE) were taken to be different two times, except for the model for VDW by the traditional schematic (at constant temperature) at different yield limits.

It is established that with the traditional VDW scheme for C–C and B–B assemblies equivalent stresses in the butt joint zone decrease in the material with lower yield limit at the moment of appearance of plastic deformations, and at further loading the portion of the component removed from the butt joint is plastically deformed (Figure 2, *a*, *b*). The butt joint in Figure 2, *a*, *b* is shown by an arrow. In B–F assembly at the same yield limits and smaller limit in the bushing, the deformation fields are similar in C–C and B–B assemblies with noticeable increase at the stress raiser (Figure 2, *c*, *d*). At a smaller yield limit of flange material, plastic deformations in it develop in a very narrow zone near the stress raiser (point *A*, Figure 1, *e*).

Modeling allowing for plastic creep deformations showed that the pattern of deformation fields does not change. With the traditional VDW scheme, plastic deformations are also absent on the greater part of the butt joint. At VDW with thermal cycling (heat-

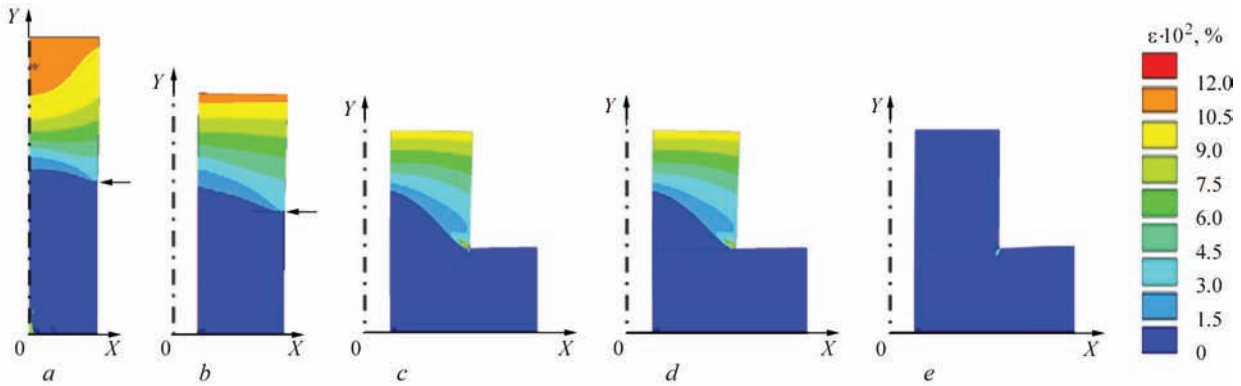

Figure 2. Fields of instantaneous plastic deformations of C–C (*a*), B–B (*b*) assemblies, at lower yield limit of part *1*, B–F assembly at equal yield limits (*c*), smaller one in the bushing (*d*) and smaller one in the flange (*e*) at the traditional scheme of VDW, allowing for instantaneous plasticity deformation

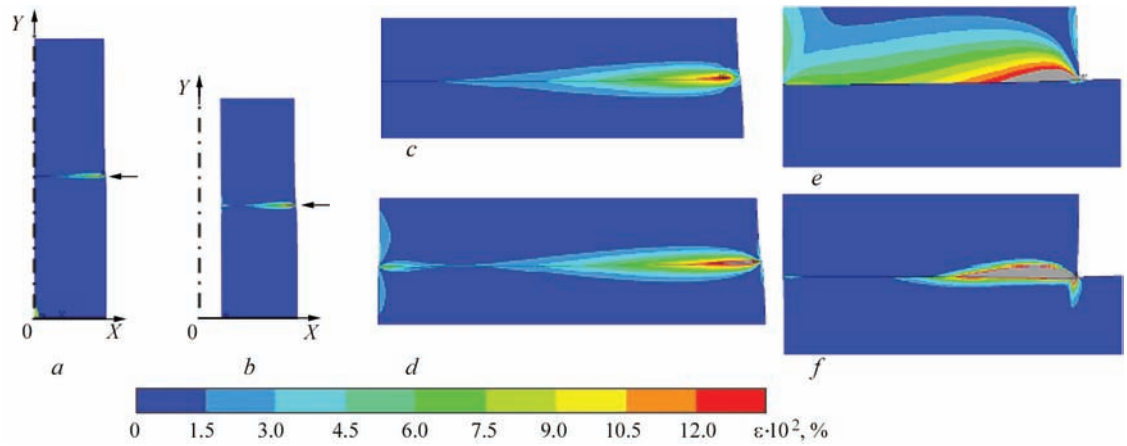

Figure 3. Fields of equivalent instantaneous plastic deformations in C–C (*a*, *c*), B–B (*b*, *d*) and B–F (*e*, *f*) assemblies with the same yield limit and smaller TCLE of parts *1* and bushing through the entire assembly (*a*, *b*) and near butt joint (*c*–*f*) at thermal loading without external pressure after adhesion of the surfaces

ing or cooling by 100 °C) without external loading by compression, after adhesion of the surfaces of C–C and B–B assemblies from materials with equal yield limits and different TCLE, ideal localizing of plastic deformations in the joint zone is achieved, covering both the materials being joined symmetrically relative to the butt joint (Figure 3, *a*–*d*). In B–F assembly at the same yield limits of bushing and flange materials the deformation fields are not symmetrical (Figure 3, *d*, *f*). Both at heating and at cooling they are concentrated near the butt joint, to a greater degree from the side of the bushing. Plastic deformations zone from the flange side much smaller. Appearance of plastic deformations reduces the peaks of all the stresses in the concentration point.

At simultaneous force (compression) and thermal (heating-cooling) loading and equal yield limits, plastic deformations increase in all the components and are more uniformly distributed in B–F assemblies. In C–C and B–B assemblies they appear alternatively in the material with smaller TCLE at heating and material with greater TCLE at cooling. If the yield limits are different, then under the modeling conditions just the material with a lower yield limit and smaller TCLE was deformed at heating.

A feature of the fields and epures of plastic deformation distribution at thermal cycling, both without external pressure, and with pressure is presence of a zone in the butt joint, where equivalent stresses and plastic deformations have minimum value, and tangential stresses and shear deformations pass through zero. It is proposed to call the point with zero tangential stresses and the surrounding zone near it with minimum equivalent stresses and deformations, the point and zone of deformation stagnation. Absence of shear deformations complicates the possibility of activation of the surfaces being joined. In C–C assembly this zone is located in its center, in B–B and B–F assemblies it is on the inner surface at the distance of approximately 0.23–0.25 of bushing thickness. Plastic deformations gradually increase from this zone to the inner and outer surface.

Effect of plastic creep deformations was studied to enhance the possibilities for SSS regulation. This was the third stage of SSS modeling (first stage for the elastic state, second stage allowing for instantaneous plasticity deformations). Here, three cycles of heating and cooling by 100 °C during 60 s with soaking for 60 s in each cycle at compressive pressure of 15 MPa were considered. Magnitude and distribution of plastic deformations after each cycle are shown in Figure 4.

During thermal cycling the stresses and plastic deformations vary by their magnitude, but the nature of their distribution along the butt joint remains the same. Material creep increases the value of plastic deformations that promotes formation of physical contact, activation of the surfaces being joined and development of recrystallization and diffusion processes, unlike the traditional VDW scheme, under the conditions of which slowly running diffusion processes have the main role [6].

VDW under the conditions of simultaneous compression and superposition of thermal cycles is more favourable for distribution of plastic deformations, ensuring their localization in the butt zone, more uniform distribution over the joint area and intensive development of the processes of joint formation.

SSS modeling was used at development of the technology of VDW of solenoid valve bodies, in which four butt joints of 12Kh18N10T (3 parts) and 10895 (2 parts) steels are welded simultaneously. Welded billet of a valve is shown in Figure 5.

Welding was conducted at total heating by high-frequency currents at three cycles of heating and cooling. As it was established by preliminary research on models, deformation occurred only at heating in the zone of butt

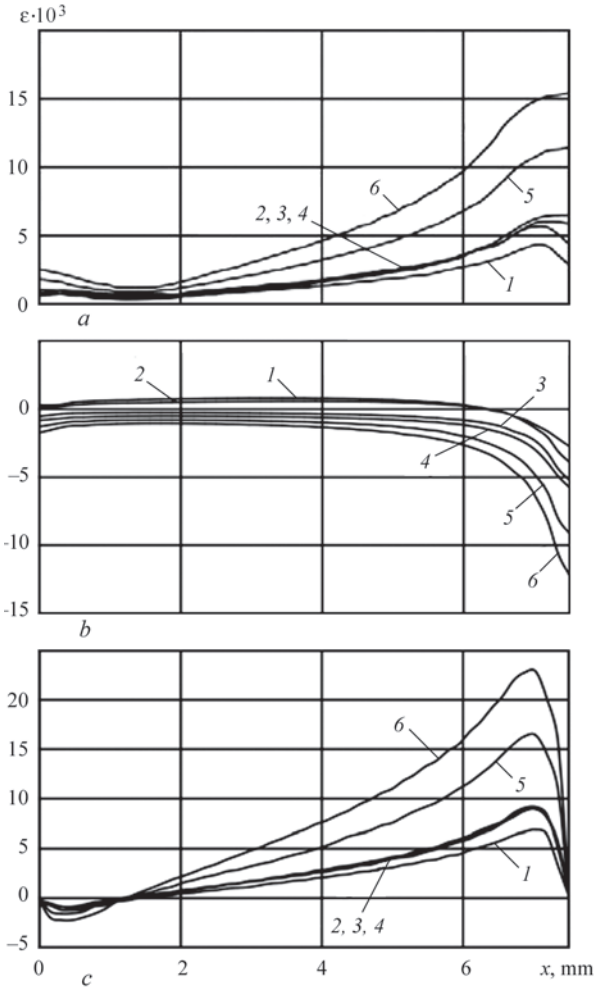

Figure 4. Epures of equivalent (*a*), axial (*b*) and shear (*c*) deformations at VDW 60 (*1*), 120 (*2*), 180 (*3*), 240 (*4*), 480 (*5*) and 720 s (*6*) after the start of thermal cycling of B–B assembly

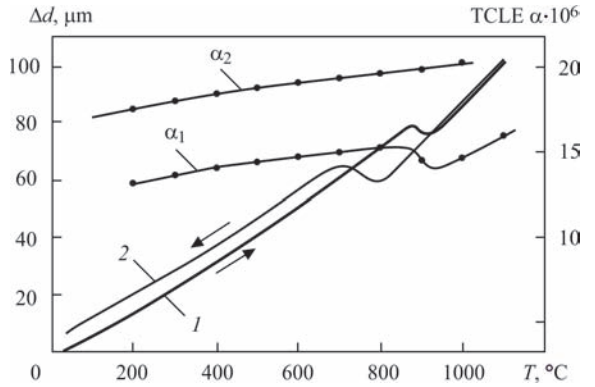

Figure 6. Dilatograms of heating (*1*) and cooling (*2*) of 10895 steel and TCLE of the same steel (α_1), and 12Kh18N10T steel (α_2)

joint of less strong 10895 steel. Measurements and result analysis were conducted after VDW.

Moduli of elasticity, yield limits, Poisson's ratios, dilatograms of heating and cooling, curves, parameters and equations of creep of the material being joined were determined as a function of temperature, in order to perform SSS modeling.

At heating 10895 steel goes from α-phase into γ-phase with the change of physicomechanical properties (PMP), in particular, with the change of TCLE, that is shown by dilatograms of heating and cooling of 10895 steel, as well as TCLE of the same steel (Figure 6). This allowed using not only temperature, but also structural deformations during thermal cycling.

Dependence of the yield limit on temperature, used at modeling, and creep curves of 10895 steel are given in Figure 7. In the thermal cycling range of 750–1050 °C the creep rate of 12Kh18N10T steel is

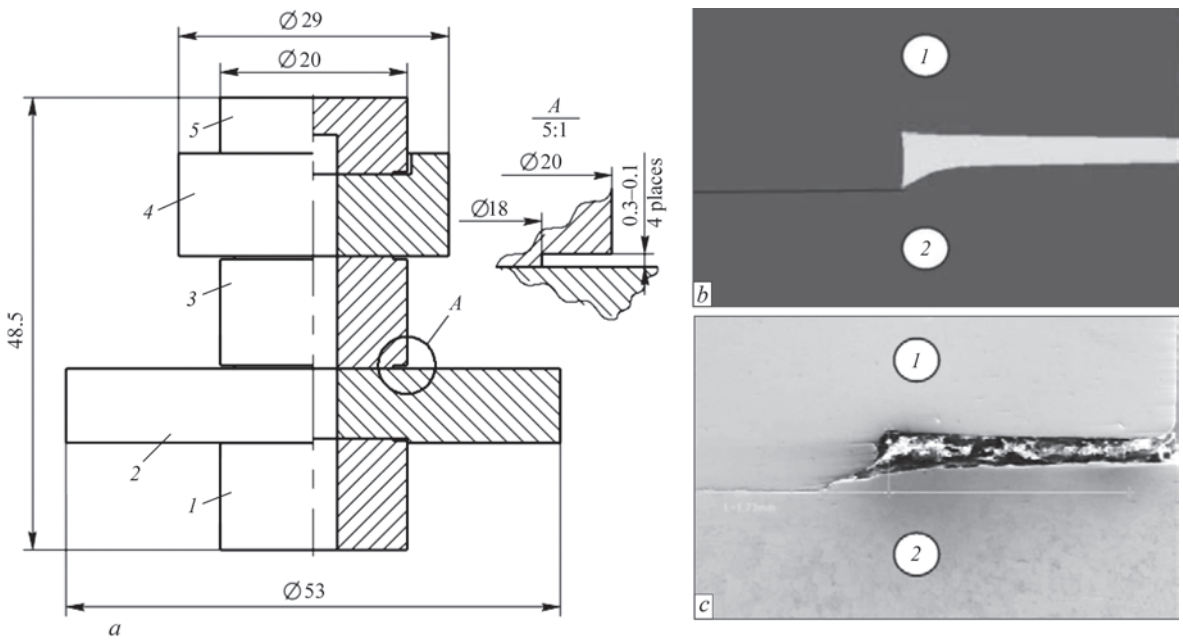

Figure 5. Welded billet of the body of the solenoid valve (*a*) and nature of billet deformation after VDW in assembly *A* of the joint of bushing *1* and flange *2* by the results of modeling (*b*) and actually (*c*): *1, 3, 5* — 12Kh18N10T steel; *2, 4* — 10895 steel

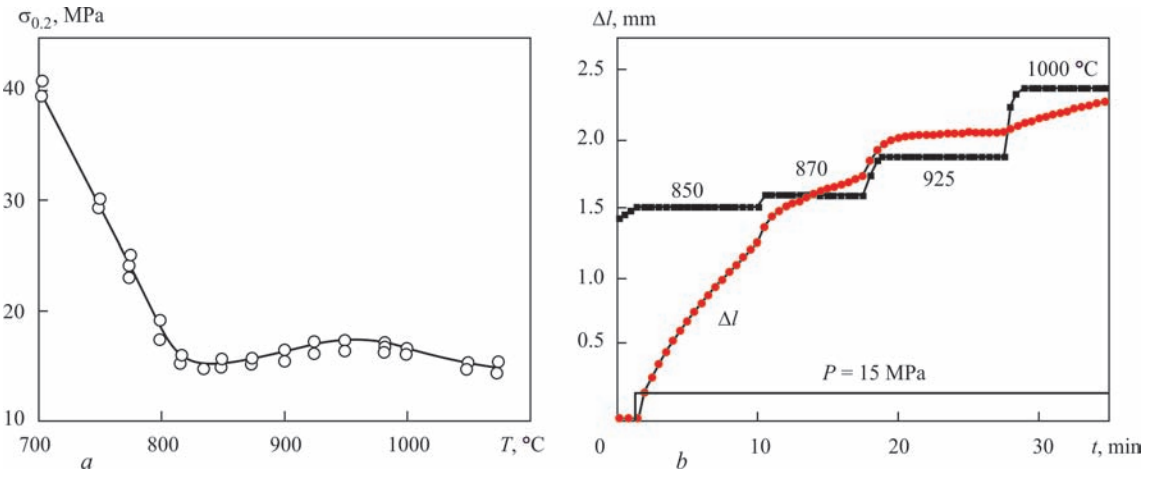

Figure 7. Influence of temperature on the yield limit (*a*) and cyclogram of creep testing of 10895 steel with the change of sample length Δ*l* at temperatures of 850, 870, 925, 1000 °C and pressure of 15 MPa (*b*)

very small, compared to 10895 steel, and its deformation can be neglected.

Creep parameters of 10895 steel were determined experimentally with application of Gleeble-3800 unit and upgraded unit for vacuum diffusion welding. Results were processed with application of an equation describing creep at the first and second stages:

$$\varepsilon = C_1 p^{C_2} \frac{t^{C_3+1}}{C_3+1} \exp\left(-\frac{C_4}{T}\right) + C_5 p^{C_6} t \exp\left(-\frac{C_7}{T}\right),$$

where ε is the deformation value; C_1–C_7 are the coefficients determined by experimental creep curves, here $C_1 > 0$; $C_3 < 0$; $C_5 > 0$; $C_4 = (\Delta H_{n(1)}/R)$; $C_7 = (\Delta H_{n(2)}/R)$; $\Delta H_{n(1)}$ and $\Delta H_{n(2)}$ is the creep activation energy at the first stage; $\Delta H_{n(2)}$ is the energy of creep activation at the second stage; C_2 and C_6 are the constants for the first and second stages, respectively.

The coefficients are determined from the series of curves, obtained for different temperatures and pressures: $C_1 = 4.99 \cdot 10^{-24}$; $C_2 = 4.59$–4.65; $C_3 = -0.32$–-0.52; $C_4 = 32700$–39800; $C_5 = 1.641 \cdot 10^{-25}$; $C_6 = 4.49$–4.95; $C_7 = 32700$–39800.

Comparison of modeling and experimental results confirmed modeling adequacy. For instance, Figure 5, *a* shows the billet configuration in the zone of the joint of bushing *3* with flange *2* in assembly *A* (see Figure 5, *b, c*). The nature of billet deformation at modeling and in the real part is the same, and quantitative values of deformations have satisfactory convergence.

Mechanical testing was also performed for experimental assessment of the effect of thermal cycling on welded joint quality. It is found that in welding without thermal cycling the samples at tensile testing failed at up to 255 MPa stresses. Fracture surface had up to 40 % of «adhesion» area, as well as the shape of a cone, that is indicative of the start of fracture in the sample center. In welding with thermal cycling three thermal cycles are sufficient to ensure equal strength of the joints with 10895 steel (more than 360 MPa). At impact bend testing cylindrical samples of 15 mm diameter did not fail at bend angle of 90°.

At testing of samples simulating the item, fracture ran in 10895 steel at stresses of (363–398)/383 MPa (mean value is given in the denominator).

To study the structure of metal in the butt zone, the method of electronic foil translucence at up to 50000 magnifications and local X-ray spectral microanalysis were used for determination of fine structure, diffusion processes and distribution of dislocation density over the butt joint area, which is due to the value and intensity of plastic deformations. Results of these studies are given in works [1, 7, 8]. The width of the diffusion zone even in the center of the cylinder, determined by distribution of chromium, nickel and iron, was equal to about 10 μm, that is significantly higher than the accepted in literature criterion of strength by the width of the diffusion zone of 3–5 μm [6]. At bench testing, the items failed with multiple margin of normative strength. Results of experimental studies confirmed the effectiveness of using not just the temperature, but also structural deformations for controlling the formation of SSS during welding.

Structural deformations were also used at VDW of dispersion-hardening high-temperature nickel alloys for joining parts, one of which was in the austenitized, and the other — in the aged condition, while thermal cycling was performed in the temperature range of 1000–1175 °C, in which the strengthening phase precipitation and dissolution occurs, and, consequently, change of the specific volume (structural deformations), that promotes development of plastic deformations in the butt joint.

The main problem of development of metal-ceramic assemblies is formation of residual SSS, associated with the difference in PMP of metal and ceramics. Here, the determinant role is played by assembly design

and processes of relaxation of stresses, arising even in matched junctions in brazing. SSS modeling allowed creating metal-ceramic assemblies without ceramics metallization with application of brazing (Figure 8).

Optimum thickness of kovar, the most critical zones of the joint, influence of deformations of instantaneous plasticity and creep on lowering of the level of residual stresses to the safe one and cooling mode were determined. Similar problems were solved at development of metal-graphite structures [9, 10].

In brazing metals to nonmetals, high-temperature nickel alloys or other similar materials, we have a joint with an interlayer, the properties and thickness of which also affect the SSS and performance of the assembly.

It is known that SSS influences mechanical properties of the material, its strength (yield limit), ductility (relative elongation) [11]. To assess this effect on the properties of the materials being joined and the interlayer in the joint zone, it is convenient to use the coefficient of stiffness of the stressed state, K_{st}, equal to the ratio of maximum modulo principal stresses to equivalent ones, $K_{st} = \sigma_{1(3)}/\sigma_{eq}$. Value of coefficient K_{st} determines the degree of softening ($K_{st} < 1$) or strengthening ($K_{st} > 1$) of the material in a specific zone of the assembly, compared to the linear stressed state, under the conditions of which standard strength testing of materials is performed.

The interlayers are divided into «stiff» and «soft». At the plastic stage of work interlayers with lower yield limit $\sigma_{int\ lim}$, than that of the base metal ($\sigma_{y\ int} < \sigma_{y\ b.m}$) belong to the soft ones, and those with greater $\sigma_{y\ int}$ ($\sigma_{y\ int} > \sigma_{y\ b.m}$) are regarded as stiff. When working in the elastic stage, the stiffness criteria are the moduli of elasticity: soft at $E_{int} < E_{b.m}$ and stiff at $E_{int} > E_{b.m}$.

Computer modeling of SSS of cylindrical assemblies with interlayers for tension and compression showed that both in the case of stiff and soft interlayer a bulk SSS with radial, hoop, axial and tangential stresses forms in a small zone of their joint with the base metal near the surface in the interlayer and adjacent regions of base metal of the width of about two interlayer thicknesses.

At tension tensile radial, hoop and axial stresses begin acting in the soft interlayer which starts deforming earlier than the base metal, while tensile axial and compressive radial and hoop stresses act in the stronger base metal. Here, the level of equivalent stresses in the interlayer decreases compared to applied load, and rises in the base metal, i.e. effect of unloading or strengthening of the interlayer and additional loading or softening of base metal is manifested [12].

In assemblies with stiff interlayer, axial tension in it is combined with compression in the radial and circumferential directions. Here, equivalent stresses in the

Figure 8. Metal-ceramic assemblies produced by brazing without ceramics metallization

interlayer increase, i.e. effect of additional loading of the interlayer or its softening is manifested [12]. That is why brittle interlayers are not allowed in brazed joints.

Computer modeling showed that at the stage of elastic deformation of the soft interlayer the coefficients of stiffness of the stressed state and strengthening of the soft interlayer and softening of the stronger base metal, respectively, depend only on the ratio of the moduli of elasticity and Poisson's ratios of the base metal and the interlayer, and do not depend on the magnitude of the applied axial load. At the plastic stage they also depend on the degree of interlayer overload, i.e. the ratio of the applied stress to the interlayer material yield limit: $K_{ov} = \sigma_l/\sigma_y$, where K_{ov} is the coefficient of interlayer overload, σ_l is the acting load on the assembly, σ_y is the interlayer material yield limit.

The uniformity of stress distribution is abruptly violated near the assembly generatrix. The epures of axial stresses along the outer surface in the zone of the butt joint of the interlayer and base metal at different axial loads at the elastic stage are shown in Figure 9, *a*, and at the elastoplastic stage — in Figure 9, *b*.

Axial stresses are nonuniformly distributed near the butt joint. At the elastic stage of the work they vary from 70 up to 120 MPa in the interlayer and from 100 up to 175 MPa in the base metal, and at the elastoplastic stage — from 90 up to 120 MPa in the interlayer and from 140 up to 255 MPa in the base metal. Maximum axial stresses essentially exceed the level of the applied external load and are present in the base metal near the butt joint. As a result, fracture can run in the stronger base metal at the junction with the in-

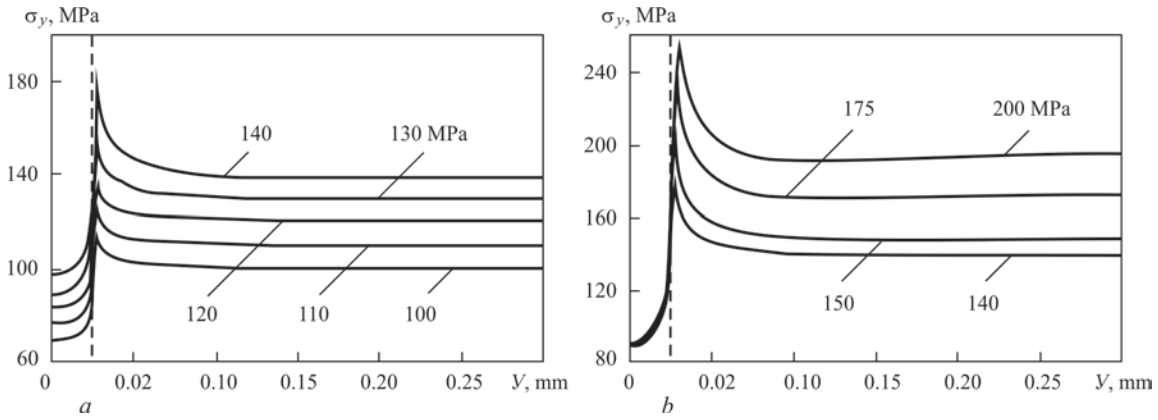

Figure 9. Epures of axial stresses along the generatrix in the zone of the butt joint of the interlayer and base metal at axial loads of 100–150 MPa (*a*) and 140–200 (*b*)

terlayer at sufficient strengthening of the soft interlayer and softening of the base metal that is confirmed by the known experiments on brazing armco-iron with copper with about 0.05 mm thickness of the copper interlayer [2].

Conclusions

1. At VDW of dissimilar materials with thermal cycling appearance of radial, axial, hoop and tangential stresses leads to formation of bulk stressed state with development of shear deformation that provides localization of plastic deformations in the butt joint zone, activation of the surfaces being joined and their active interaction over the entire area. The nature and level of SSS are to the greatest extent determined by the external compressive pressure, difference in TCLE, temperature variation range and structural deformations. For instance, plastic deformation is localized in the zone of the butt joint at VDW of dispersion-hardened high-temperature nickel alloys, which are in the aged and austenitized states, α- to γ-phase transitions, etc.

2. At high-temperature brazing of nonmetallized ceramics with kovar deformations of instantaneous plasticity in the high-temperature and creep range at lower temperatures allow decreasing the residual stresses in metal-ceramic assemblies below the ultimate tensile strength of the ceramics. The mode of cooling under pressure promotes stress relaxation.

3. In the joints of similar metals with a soft interlayer, a bulk SSS forms in the butt joint zone at application of axial load. It changes the characteristics of strength and ductility of the metal, obtained at testing under the conditions of linear stressed state that promotes appearance of the effect of interlayer material strengthening and softening of the stronger base metal. Maximum axial stresses develop in the base metal near the butt joint that, in combination with softening, can lead to joint fracture in the stronger base metal.

1. Krivtsun, I.V., Kvasnytskyi, V.V., Maksymov, S.Yu., Ermolayev, H.V. (2017) Special methods of welding. Ed. by B.E. Paton. Mykolaiv, NUK [in Ukrainian].
2. Ermolayev, H.V., Kvasnytskyi, V.V., Kvasnytskyi,V.F. et al. (2015) *Brazing of materials*. Ed. by V.F. Khorunov et al. Mykolaiv, NUK [in Ukrainian].
3. Makhnenko, V.I., Kvasnitsky, V.F. (2009) Peculiarities of formation of stress-strain state in diffusion bonds between dissimilar materials. *The Paton Welding J*., **8**, 7–11.
4. Kvasnytskyi, V.V., Ermolayev, H.V., Matvienko, M.V. (2017) *Mechanics of joints in diffusion welding, brazing and spraying of dissimilar materials under elasticity conditions*. Nikolaev, NUK [in Russian].
5. Kvasnitsky, V.V., Zolotoj, Yu.G., Labartkava, A.B. et al. (2008) *Experimental investigation of deformation of welded assembly of bush-bush type from dissimilar materials*: Transact. NUK, Mykolaiv, NUK, 4, 65–73 [in Russian].
6. Kazakov, N.F. (1976) *Diffusion welding of materials*. Moscow, Mashinostroenie [in Russian].
7. Lobanov, L.M., Ermolayev, H.V., Kvasnytskyi, V.V. et al. (2016) *Stresses and strains in welding and brazing*. Ed. by L.M. Lobanov. Mykolaiv, NUK [in Ukrainian].
8. Kvasnitsky, V.V., Kvasnitsky,V.F., Markashova, L.I., Matvienko, M.V. (2014) Effect of stress-strain state on structure and properties of joints in diffusion welding of dissimilar metals. *The Paton Welding J*., **8**, 8–14.
9. Emelyanov, V.M., Kvasnytskyi, V.V., Ermolayev, H.V. et al. (2009) Optimization of structure of metal-graphite slidebearings on the base of residual stresses analysis in brazed assemblies. *Vestnik Khersonsk. NTU*, **3**, 42–46 [in Russian].
10. Ermolaev, G.B., Martynenko, V.A., Olekseenko, S.V. et al. (2017) Effect of the rigid interlayer thickness on the stressstrain of metal-grafite assemblies under thermal loading. *Strength of Materials*, May, 49(**3**) 422–428.
11. Kopelman, L.A. (2010) *Principles of theory of strength of welded structures*. St.-Petersburg, Lan [in Russian].
12. Kvasnytskyi, V.V., Kvasnytskyi,V.F., Dong Chunlin, Matvienko, M.V. et al. (2018) Stressed state of welded and brazed assemblies from similar materials with a soft interlayer under axial loading. *The Paton Welding J*., **4**, 6–10.

Received 30.03.2018